

FINITE ELEMENT MODELING AND SIMULATION OF VISCOUS MEMBRANES

Italo V. Tasso and Gustavo C. Buscaglia

*Instituto de Ciências Matemáticas e de Computação, Universidade de São Paulo, Av. do Trabalhador
São-carlense 400, 13560-970 São Carlos, SP, Brazil, <http://www.lcad.icmc.usp.br/~buscaglia>*

Keywords: Elastic membrane, viscous membrane, cytoskeleton, lipidic bilayer, inextensibility, Canham-Helfrich energy, finite elements.

Abstract. Fluid membranes and, in particular, lipidic bilayers play a fundamental role in the structure of eukaryotic cells. These membranes change shape and topology according to different cell functions, and their dynamics affects the pace of physiological processes. Much attention has recently been devoted to the study of fluid membranes in the mathematical literature, and advances have been made in the numerical treatment of the membrane/fluid interaction and of the bending stiffness of the membranes, as modeled by means of the Canham-Helfrich energy. In this contribution we discuss the different aspects of viscous membrane simulations, and then focus in the issue of the tangential behavior of the membrane. In its simplest form, the problem reduces to that of the two-dimensional flow of a Stokesian fluid on a time-evolving surface, which has scarcely been discussed in the literature. The membrane fluid is assumed inextensible, meaning that elementary surface areas are preserved throughout the motion. A suitable variational formulation is discussed and its discretization by finite elements presented, together with illustrative examples.

1 INTRODUCTION

Fluidic behavior is characterized by the impossibility of rest under shear. In Nature, as well as in the biomedical industry, there exist highly-deformable membranes that exhibit fluidic behavior. This is the case of lipidic bilayers, which are a basic constituent of the living cell membrane. They consist of two molecular layers of lipids, each layer exposing the hydrophilic ends of their molecules to the adjacent water and thus also keeping the hydrophobic ends away from it. The molecules in lipidic membranes exhibit very high tangential mobility, with relatively low layer-to-layer transfer rate. This qualifies the membrane as a two-dimensional fluid, flowing on a time-dependent, curved surface in three-dimensional space.

The actual rheological behavior of lipidic bilayers is predominantly viscous (Seifert, 1997; Lipowsky, 1991; Mader et al., 2006) with a surface viscosity of about 5×10^{-9} Pa-s-m (Vaughn, 1982) that can take higher values, up to 2×10^{-6} Pa-s-m. Though some viscoelasticity may exist, recent rheometrical data suggest that it is not significant (Harland et al., 2010, 2011). The surface viscous effects, in turn, can predominate over the bulk viscous effects in the less mobile regimes (Cicuta et al., 2007).

In this work we propose a novel method for the finite element simulation of viscous membranes. It is strongly based on the well-established finite element treatment of *elastic* membranes, which is briefly reviewed first (see Holzapfel et al. (1996) for details; and Ramanujan and Pozrikidis (1998); Lac and Barthès-Biesel (2005); Sui et al. (2009); Li and Sarkar (2008); Le et al. (2009) for biological applications). In a suitable limit, the elastic operator tends to the viscous operator, to which we add the zero-tangential-divergence (inextensibility) condition to arrive at a complete model. This latter condition introduces a Lagrange multiplier field P (in fact, a non-homogeneous surface tension). A stabilization term proportional to the surface Laplacian of P is added to allow for the use of the same interpolants for all fields. Overall, the method seems to be the first to compute truly viscous and inextensible relaxation of membranes in general 3D geometries. Possible applications of the proposed method are numerous, such as studies of membrane adhesion (Das and Du, 2008) or conformation (Lipowsky, 1991), among many others.

2 ELASTIC MEMBRANES

2.1 Membrane kinematics

The large-deformation kinematics of membranes is already well studied. The interested reader is referred, for example, to the detailed article by Holzapfel et al. (1996). The deformation, at some instant t , of the material points of the membrane is described by the right tangential Cauchy-Green tensor \mathbb{C}^t . The energy density of an isotropic elastic material is a function of the invariants of \mathbb{C}^t (such as its eigenvalues, λ_1^2 and λ_2^2). If the deformation preserves area, then $\det(\mathbb{C}^t) = \lambda_1^2 \lambda_2^2 = 1$. Also notice that the first invariant (the trace) is given by $\text{tr}(\mathbb{C}^t) = \lambda_1^2 + \lambda_2^2$.

To compute the elastic energy of an isotropic material, let us assume transformations of the form

$$\varphi(\boldsymbol{\xi}) = \sum_{m=1}^M \mathbf{X}_{(m)} N_{(m)}(\boldsymbol{\xi}) \quad (1)$$

For Lagrangian finite elements, clearly, $\{N_{(m)}\}$ is the set of basis functions on the master (unit) element. Since the elastic energy E_e depends on both the reference configuration $\underline{\mathbf{Y}}$ and the

current configuration (time t), we write it as

$$E_e(\underline{\mathbf{Y}}, \underline{\mathbf{X}}^t) = \int_{\Gamma} \rho e_e d\Gamma \quad (2)$$

with ρ the surface mass density. For a Mooney–Rivlin material, for example,

$$e_e = c_1 (\lambda_1^2 + \lambda_2^2 - 2) + c_2 (\lambda_1^2 \lambda_2^2 - 1) \quad (3)$$

2.2 Elastic membrane dynamics: Virtual work principle

Considering just the elasticity of the membrane and its inertia, the virtual work principle states that the virtual power of the internal forces equals the virtual power of the acceleration. Since the internal forces are elastic, their virtual power equals minus the derivative of the elastic energy with respect to the geometrical degrees of freedom $\underline{\mathbf{X}}$, that is

$$\lim_{\epsilon \rightarrow 0} \frac{E_e(\underline{\mathbf{Y}}, \underline{\mathbf{X}}^t + \epsilon \underline{\mathbf{w}}) - E_e(\underline{\mathbf{Y}}, \underline{\mathbf{X}}^t)}{\epsilon} + \int_{\Gamma(t)} \rho \underline{\mathbf{a}} \cdot \underline{\mathbf{w}} d\Gamma = 0 \quad (4)$$

where the configuration $\underline{\mathbf{X}}^t + \epsilon \underline{\mathbf{w}}$ is defined by perturbing the position of the interface along the virtual velocity field $\underline{\mathbf{w}}$ and $\underline{\mathbf{a}}$ is the acceleration.

Though the first term of (4) may be represented as a distribution of forces on the membrane, we for later use leave the computation of the elastic term as the limit of finite differences. We emphasize that (4) is a non-linear system of ordinary differential equations for the unknowns $\underline{\mathbf{X}}^t$:

$$\lim_{\epsilon \rightarrow 0} \frac{E_e(\underline{\mathbf{Y}}, \underline{\mathbf{X}}^t + \epsilon \underline{\mathbf{D}}_{(i,m)}) - E_e(\underline{\mathbf{Y}}, \underline{\mathbf{X}}^t)}{\epsilon} + \sum_{\ell=1}^M \left[\int_{\Gamma(t)} \rho N_{(\ell)} N_{(m)} d\Gamma \right] \frac{d^2 X_{(\ell)i}^t}{dt^2} = 0 \quad (5)$$

where $X_{(\ell)i}^t$ is the i -th coordinate, at time t , of node ℓ and (5) must hold for all m and i . The perturbation $\underline{\mathbf{D}}_{(i,m)}$ corresponds to a unit movement of node m along coordinate i . The bracketed term is the usual mass matrix on $\Gamma(t)$, with components $A_{k\ell}$. If the mass of the membrane is conserved ($\rho d\Gamma$ independent of t) the mass matrix does not depend on time.

2.3 Effect of the surrounding fluid

To consider the full effect of the surrounding fluid, the 3D Navier–Stokes equations coupled to (5) need to be solved, incorporating the forces exerted by the fluid. If inertia is neglected, the boundary element formulation based on fundamental solutions of the Stokes equations has gained much popularity (Ramanujan and Pozrikidis, 1998; Pozrikidis, 2003; Li and Sarkar, 2008). We leave this issue outside the scope of this article, limiting the discussion to the incorporation of gravitational energy. Assume the membrane contains a fluid of constant density ρ_ℓ and that gravity is also constant (equal to $-g \check{\mathbf{e}}_3$). Then the gravitational energy of the membrane together with that of the enclosed fluid is given by

$$E_{\text{grav}} = \int_{\Gamma(t)} \left(\rho x_3 + \rho_\ell \frac{x_3^2}{2} n_3 \right) g d\Gamma \quad (6)$$

Further, assume that the internal fluid is pressurized to some pressure $p(t)$, assumed known. Since the work of this pressure upon a virtual change in volume is $p(t) \Delta \mathcal{V}$, for virtual work

calculations the term $-p(t) \mathcal{V}(\underline{\mathbf{X}}^t)$ needs to be added. If, on the other hand, the volume $\mathcal{V}(\underline{\mathbf{X}}^t)$ enclosed by the membrane is imposed, for example because the inner fluid is incompressible, then the internal pressure $p(t)$ becomes an unknown (Lagrange multiplier). Denoting by $\bar{\mathcal{V}}(t)$ the imposed value, the additional equation is

$$\mathcal{V}(\underline{\mathbf{X}}^t) = \bar{\mathcal{V}}(t) \quad (7)$$

and the dynamic effect can be incorporated into the energy by adding the term

$$-p(t) [\mathcal{V}(\underline{\mathbf{X}}^t) - \bar{\mathcal{V}}(t)] \quad (8)$$

2.4 Obstacles and contact

The presence of unilateral constraints such as solid obstacles can also be accounted for in the energy. In this work we adopt a simple penalty approach of the form

$$E_{\text{con}} = \int_{\Gamma(t)} \frac{\alpha_{\text{con}}}{2} \delta^2 d\Gamma \quad (9)$$

where δ is the *penetration depth* of the membrane into the solid obstacle. The contact of the membrane with itself (self penetration) can be dealt with in the same way.

2.5 An algorithm for elastic membranes

Gathering the results of the previous sections it is possible to build a complete algorithm for the simulation of elastic membranes. For nodal positions $\underline{\mathbf{X}}$ of the membrane, we consider the energy

$$\mathcal{E} = E_e(\underline{\mathbf{Y}}, \underline{\mathbf{X}}) + E_{\text{grav}}(\underline{\mathbf{X}}) + E_{\text{con}}(\underline{\mathbf{X}}) - p [\mathcal{V}(\underline{\mathbf{X}}) - \bar{\mathcal{V}}] \quad (10)$$

and assume $\bar{\mathcal{V}}$ to be a given function of time, so that $p(t)$ is unknown (the case in which $p(t)$ is given is easier). The relaxed configuration $\underline{\mathbf{Y}}$ is given *and fixed*. Also given is the initial nodal-velocity vector $\underline{\mathbf{U}}^0$.

Continuous-in-time discrete problem: For $t > 0$, find $(\underline{\mathbf{X}}^t, \underline{\mathbf{U}}^t, p(t))$ such that for all i, m and δp ,

$$\frac{d\underline{\mathbf{X}}^t}{dt} - \underline{\mathbf{U}}^t = 0 \quad (11)$$

$$\frac{\mathcal{E}(\underline{\mathbf{Y}}, \underline{\mathbf{X}}^t + \epsilon \underline{\mathbf{D}}_{(i,m)}, p(t)) - \mathcal{E}(\underline{\mathbf{Y}}, \underline{\mathbf{X}}^t, p(t))}{\epsilon} + \sum_{\ell=1}^M A_{m\ell} \frac{dU_{(\ell)i}^t}{dt} = 0 \quad (12)$$

$$\mathcal{E}(\underline{\mathbf{Y}}, \underline{\mathbf{X}}^t, p(t) + \delta p) - \mathcal{E}(\underline{\mathbf{Y}}, \underline{\mathbf{X}}^t, p(t)) = 0 \quad (13)$$

The equations above constitutes a system of $6M + 1$ differential-algebraic equations that can be solved by standard methods. Notice that the only algebraic equation is (13), which is in fact another way of writing the constraint (7).

2.6 Time discretization

For the purpose of illustrating the method, we implemented two numerical schemes for (11)-(13), an explicit fourth-order Runge-Kutta scheme and a fully-implicit backward Euler scheme that will later on be extended to deal with viscous membranes.

Runge-Kutta scheme: Let $\mathbb{X} = (\underline{\mathbf{X}}, \underline{\mathbf{U}})$ be the array of nodal positions and velocities, and let \mathbb{X}^n and p^n be the already calculated unknowns at time t_n . Then, for each tentative value p^* of the pressure at time t_{n+1} , and by performing one time step of the Runge-Kutta scheme for equations (11)-(12), one obtains a different \mathbb{X}^{n+1} . Formally, this can be written as

$$\mathbb{X}^{n+1}(p^*) = (\underline{\mathbf{X}}^{n+1}(p^*), \underline{\mathbf{U}}^{n+1}(p^*)) \quad (14)$$

The correct value of p^{n+1} is thus obtained by solving the volume-constraint equation

$$\mathcal{V}(\underline{\mathbf{X}}^{n+1}(p^{n+1})) = \bar{\mathcal{V}}(t_{n+1}) \quad (15)$$

Backward-Euler scheme: In this case we simply discretize the time derivatives by backward differences transforming (11)-(13) into a nonlinear algebraic system. This system is then solved by Newton-Raphson iterations with a finite-difference evaluation of the Jacobian matrix.

2.7 A numerical example

Figure 1 shows a fluid-filled membrane under gravity interacting with several cylindrical obstacles. The initial radius is $R = 1$, the membrane mass is $M = 1$ and the density of the internal fluid is $\rho_f = 1$, under unit gravity $g = 1$. The material is Hookean with $\mu = 1$ and $\lambda = 2$.

3 VISCOUS MEMBRANES

3.1 Surface viscous behavior

A classical derivation of the viscous operator from conservation principles can be found in the pioneering article by [Scriven \(1960\)](#). A geometric form of the operator in the language of differential forms is derived in the article by [Arroyo and DeSimone \(2009\)](#), with interesting two-dimensional examples of budding. The resulting equations turn out to be quite involved, with the additional complication of depending explicitly on the hard-to-discretize curvature tensor. As a consequence, no general numerical algorithm is available for the dynamic simulation of three-dimensional viscous membranes. Most existing methodologies focus on the obtention of the equilibrium state by gradient flow ([Feng and Klug, 2006](#); [Ma and Klug, 2008](#); [Dziuk, 2008](#); [Bonito et al., 2010](#)), disregarding the relaxation dynamics. Others compute the damping effect of the surrounding fluid but neglect the surface viscous effects ([Bonito et al., 2011](#)).

The approach we propose here is based on Maxwell's idea of viewing viscosity as "fugitive elasticity". It is best explained considering an elastic spring for which the force depends on the current position x , on the elastic constant k and on the equilibrium position a as

$$F(k, a; x) = -k(x - a) \quad (16)$$

Defining the energy $E(k, a; x) = \frac{1}{2}k(x - a)^2$ it is readily seen that

$$F = -\lim_{\delta \rightarrow 0} \frac{E(k, a; x + \delta) - E(k, a; x)}{\delta} \quad (17)$$

so that the forces can be computed using (17) for some sufficiently small δ . Now assume that one wants to compute a viscous spring, i.e.; a spring satisfying

$$F = -\mu V, \quad (18)$$

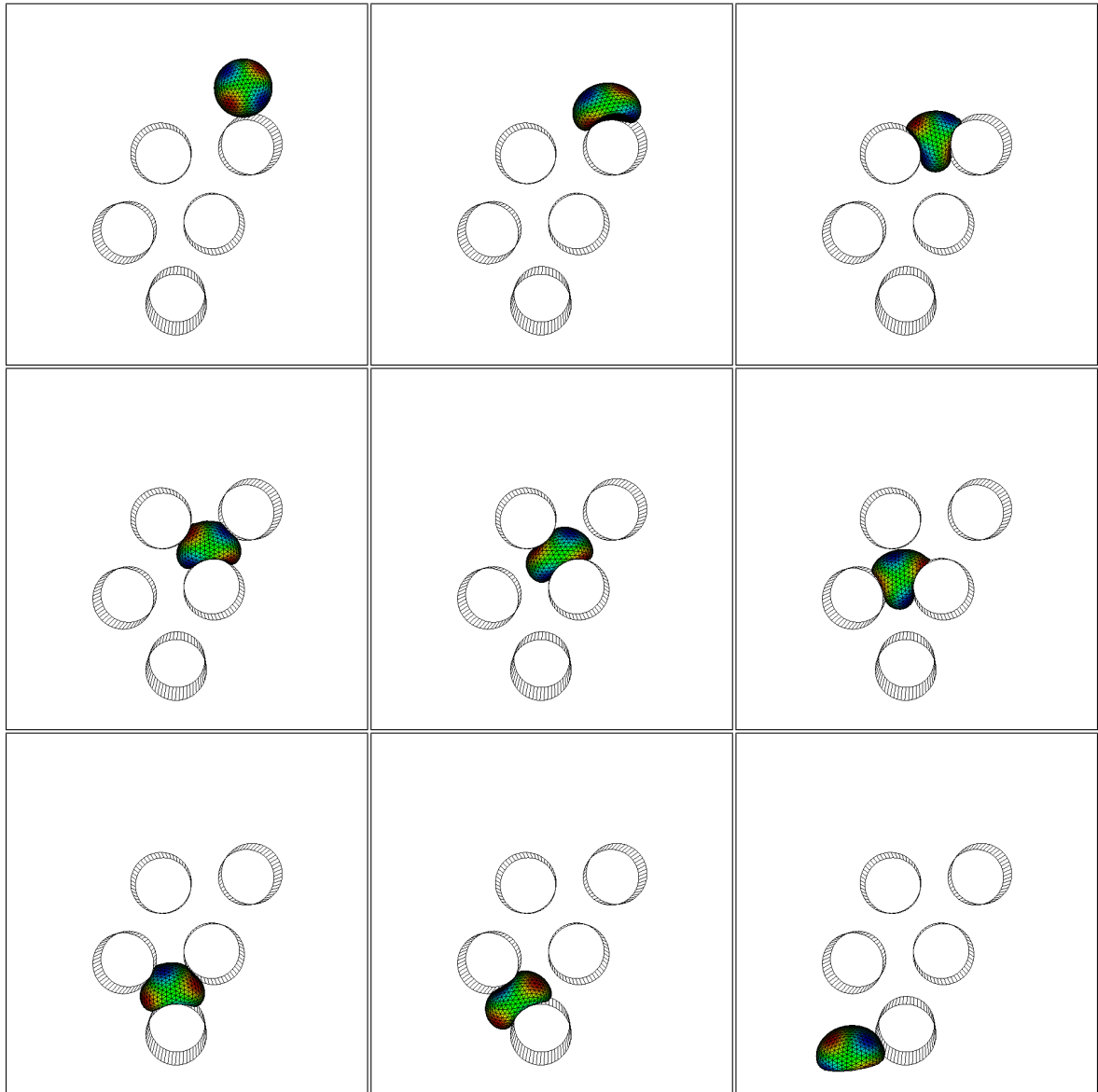


Figure 1: Elastic membrane under gravity interacting with solid obstacles.

where $V = dx/dt$ is the velocity, using the code developed for the elastic spring above. Consider the elastic energy that results from taking the equilibrium position as $a = x - V\tau$, for some small time interval τ , and with elastic constant $k = \mu/\tau$. Substituting into (17) one obtains

$$F = -\lim_{\delta \rightarrow 0} \frac{E\left(\frac{\mu}{\tau}, x - V\tau; x + \delta\right) - E\left(\frac{\mu}{\tau}, x - V\tau; x\right)}{\delta} = -\mu V \quad (19)$$

which shows that the viscous behavior can be reproduced as the elastic behavior with reference configuration $x - V\tau$ and elastic constant μ/τ , for τ sufficiently small.

The same procedure, also used by Ma and Klug in their “viscous regularization” of mesh movement (Ma and Klug, 2008), is adopted to discretize the viscous operator. The approximate viscous operator is thus given by

$$\mathcal{A}(\mathbf{X}^t, \mathbf{U}^t; \mathbf{w}) \simeq \frac{E_e(\mathbf{X}^t - \tau \mathbf{U}^t, \mathbf{X}^t + \epsilon \mathbf{w}) - E_e(\mathbf{X}^t - \tau \mathbf{U}^t, \mathbf{X}^t)}{\epsilon} \quad (20)$$

where the elastic energy must correspond to a material having shear modulus $G = \mu/\tau$. Notice that when embedding the operator above into a time-stepping scheme it is possible to take $\tau = \Delta t$ and thus $\mathbf{X}^t - \tau \mathbf{U}^t \simeq \mathbf{X}^{t-\Delta t}$, which amount to taking the previously computed configuration as reference configuration. We however leave τ as a free parameter to be tuned later on. This also emphasizes the velocity dependence of the viscous term, which would be hidden into $\mathbf{X}^{t-\Delta t}$ otherwise.

3.2 The inextensibility condition

It is well-established that lipidic bilayers tend to be *inextensible*, in the sense that the area of every part of the surface is preserved under deformation. In most simulations up to now this condition has only been imposed *globally* (Feng and Klug, 2006; Ma and Klug, 2008; Dziuk, 2008; Bonito et al., 2010), requiring that the total area is preserved.

Here we enforce (weakly) the inextensibility condition throughout the surface. For this purpose, we express the condition as

$$\int_{\Gamma(t)} Q (d\Gamma - d\Gamma_{\mathbf{Y}}) = 0 \quad \forall Q \in L^2(\Gamma(t)) \quad (21)$$

where $d\Gamma_{\mathbf{Y}}$ is the area differential in the reference configuration \mathbf{Y} . This constraint defines a lagrange-multiplier field P^t on $\Gamma(t)$, which plays the role of an unknown surface tension and whose virtual work must be accounted for in the momentum equation. Once again, this can be incorporated into the global energy from which the forces are computed by perturbation. The term to be added is linear in P^t and reads

$$\mathcal{B}(\mathbf{Y}, \mathbf{X}^t; P^t) = - \int_{\Gamma(t)} P^t (d\Gamma - d\Gamma_{\mathbf{Y}}) \quad (22)$$

3.3 Stabilization of the inextensibility constraint

Equation 21 is equivalent to

$$\int_{\Gamma(t)} Q \operatorname{div}_{\Gamma} \mathbf{u} d\Gamma = 0 \quad (23)$$

where $\operatorname{div}_{\Gamma}$ is the *surface divergence* operator and \mathbf{u} the Eulerian velocity field. In simple words, inextensibility is nothing but two-dimensional incompressibility of the membrane material considered as a surface fluid. It is thus not surprising that, when discretizing (21) with finite elements of the same polynomial degree for \mathbf{X} , \mathbf{U} and P , violent oscillations appear in P indicative of spurious modes. To stabilize the formulation, we add a P -surface diffusion term which turns (21) into

$$\int_{\Gamma(t)} Q (d\Gamma - d\Gamma_{\mathbf{Y}}) + \int_{\Gamma(t)} \zeta \nabla_{\Gamma} P \cdot \nabla_{\Gamma} Q d\Gamma = 0 \quad (24)$$

where ζ is a mesh-dependent parameter taken as

$$\zeta = \frac{h^2}{4\mu} \quad (25)$$

3.4 Bending energy of viscous membranes

It is quite intuitive that inertial and gravitational forces do not play a significant role in the biological interfaces modeled as viscous membranes. This leaves the model presented up to now with no driving force to generate motion, making any initial configuration a trivial solution.

Let us thus add a bending component to the previous ingredients, so that the membrane will be driven towards minimizers of the bending energy. The most accepted model is the Canham–Helfrich energy (Canham, 1970; Helfrich, 1973), which in its simplest form is given by

$$E_{CH} = \frac{C_{CH}}{2} \int_{\Gamma(t)} \kappa^2 d\Gamma \quad (26)$$

with κ the mean curvature of the surface and C_{CH} a dimensional constant.

It is not obvious how to discretize (26), since obviously a convergent approximation for κ in $L^2(\Gamma(t))$ must be devised. We refer to the literature (Feng and Klug, 2006; Ma and Klug, 2008; Dziuk, 2008; Bonito et al., 2010) for some options. In this work, since the emphasis is on the viscous and incompressibility operators, we adopted the discretization of κ proposed by Meyer et al. (2002), leaving further improvements on this topic for later work.

3.5 An algorithm for viscous membranes

Summing up the several contributions defined in the previous sections and neglecting inertial and gravitational terms, an algorithm for viscous membranes reads:

Initial data and mesh: Given an initial mesh of linear triangles that, in particular, provides $\underline{\mathbf{X}}^0$, and assuming continuous P_1 interpolation for all fields.

Time stepping: For $\underline{\mathbf{X}}^n$ given, compute $\underline{\mathbf{X}}^{n+1}$, $\underline{\mathbf{U}}^{n+1}$, p^{n+1} and P^{n+1} satisfying, for all i , m and Q :

$$\frac{\underline{\mathbf{X}}^{n+1} - \underline{\mathbf{X}}^n}{\Delta t} - \underline{\mathbf{U}}^{n+1} = 0 \quad (27)$$

$$\frac{\mathcal{E}(\underline{\mathbf{Y}}, \underline{\mathbf{X}}^{n+1} + \epsilon \underline{\mathbf{D}}_{(i,m)}, p^{n+1}, P^{n+1}) - \mathcal{E}(\underline{\mathbf{Y}}, \underline{\mathbf{X}}^{n+1}, p^{n+1}, P^{n+1})}{\epsilon} = 0 \quad (28)$$

$$\mathcal{V}(\underline{\mathbf{X}}^{n+1}) - \bar{\mathcal{V}}(t_{n+1}) = 0 \quad (29)$$

$$\mathcal{B}(\underline{\mathbf{Y}}, \underline{\mathbf{X}}^{n+1}; Q) + \int_{\Gamma^{n+1}} \zeta \nabla_{\Gamma} P^{n+1} \cdot \nabla_{\Gamma} Q d\Gamma = 0 \quad (30)$$

where $\underline{\mathbf{Y}} = \underline{\mathbf{X}}^{n+1} - \tau \underline{\mathbf{U}}^{n+1}$ and

$$\mathcal{E}(\underline{\mathbf{Y}}, \underline{\mathbf{X}}, p, P) = E_e(\underline{\mathbf{Y}}, \underline{\mathbf{X}}) + E_{CH}(\underline{\mathbf{X}}) - p[\mathcal{V}(\underline{\mathbf{X}}) - \bar{\mathcal{V}}(t)] + \mathcal{B}(\underline{\mathbf{Y}}, \underline{\mathbf{X}}, P) \quad (31)$$

3.6 A numerical example

In Figure 2 we show the evolution towards a local minimum of E_{CH} of a membrane which initially is an axisymmetric ellipsoid of aspect ratio 4:4:1. The final state corresponds to the well-known biconcave shape.

4 CONCLUSIONS

A novel numerical method has been proposed for the numerical simulation of viscous membranes. It is based upon well-established methodologies for elastic membranes, and the viscous

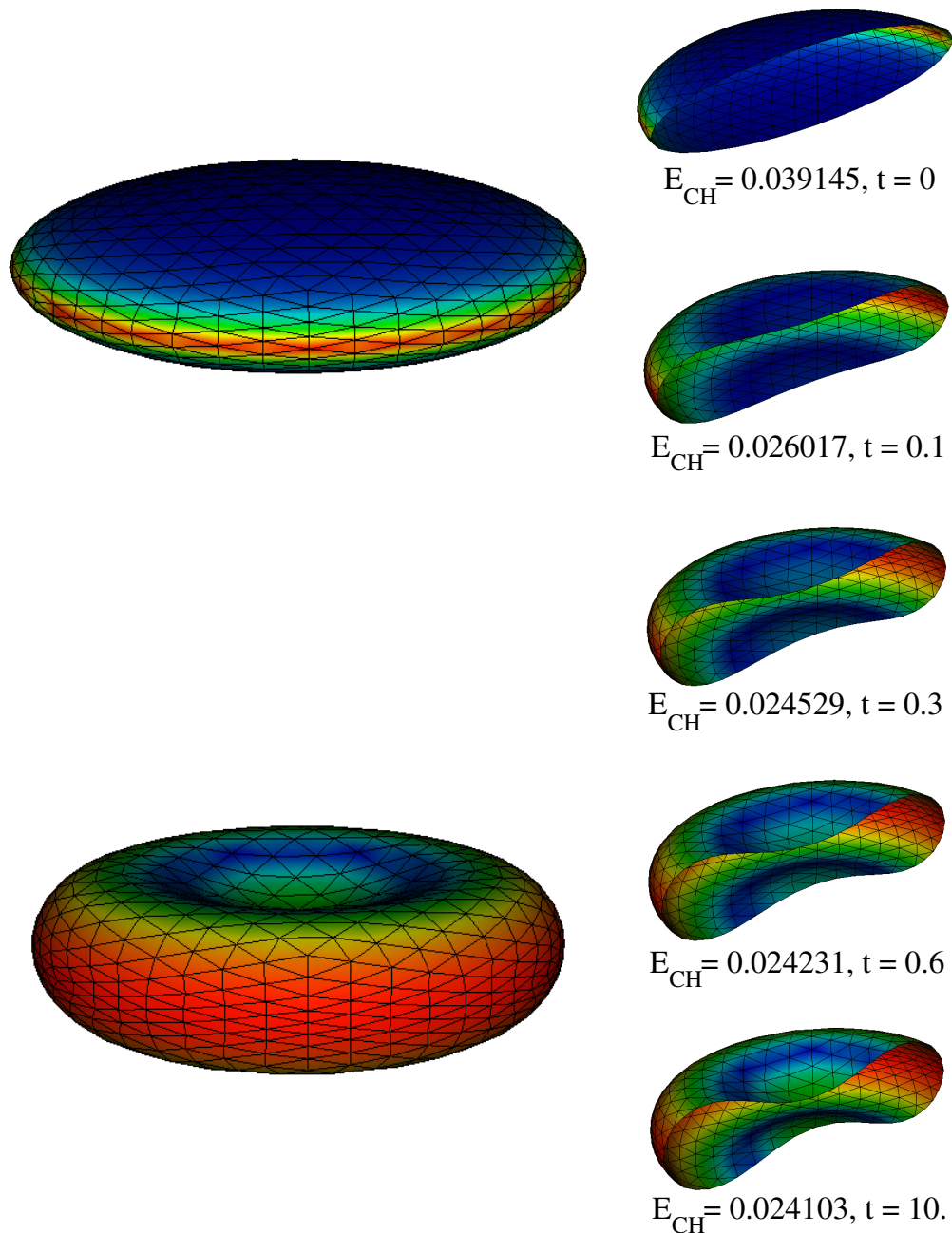


Figure 2: Viscous membrane evolving towards the minimum of the Canham–Helfrich energy, with an axisymmetric ellipsoid as initial state. Shapes colored with curvature value for different times. Also notice the value of E_{CH} for each shape.

behavior is obtained as the limit of evanescent memory. The inextensibility constraint is imposed by Lagrange multipliers, stabilized by a mesh–dependent diffusion term. The proposed method is the first one that allows for the prediction of the relaxation dynamics of lipidic bilayers of general, three–dimensional shape. Further work is in progress to assess the method in detail, optimize its parameters, and apply it to more realistic situations.

ACKNOWLEDGEMENTS

This work was partially supported by the Brazilian agencies CAPES, CNPq and FAPESP. The support of these agencies is gratefully acknowledged. The authors thank Q. Du for useful comments and suggestions.

REFERENCES

- Arroyo M. and DeSimone A. Relaxation dynamics of fluid membranes. *Physical Review E*, 79:031915 (17 pages), 2009.
- Bonito A., Nochetto R., and Pauletti S. Parametric FEM for geometric biomembranes. *Journal of Computational Physics*, 229:3171–3188, 2010.
- Bonito A., Nochetto R., and Pauletti S. Dynamics of biomembranes: Effect of the bulk fluid. *Math. Model. Nat. Phenom.*, 6:25–43, 2011.
- Canham P. The minimum energy of bending as a possible explanation of the biconcave shape of the human red blood cell. *J. Theoretical Biology*, 26:61–81, 1970.
- Cicuta P., Keller S., and Veach S. Diffusion of liquid domains in lipid bilayer membranes. *J. Phys. Chem. B*, 111:3328–3331, 2007.
- Das S. and Du Q. Adhesion of vesicles to curved substrates. *Phys. Rev. E*, 77:011907, 2008.
- Dziuk G. Computational parametric Willmore flow. *Numer. Math.*, 111:55–80, 2008.
- Feng F. and Klug W. Finite element modeling of lipid bilayer membranes. *J. Comput. Phys.*, 220:394–408, 2006.
- Harland C., Bradley M., and Parthasarathy R. Phospholipid bilayers are viscoelastic. *Proc. Natl. Acad. Sci. USA*, 107:19146–19150, 2010.
- Harland C., Bradley M., and Parthasarathy R. Retraction. *Proc. Natl. Acad. Sci. USA*, www.pnas.org/cgi/doi/10.1073/pnas.1111381108, 2011.
- Helfrich W. Elastic properties of lipid bilayers – theory and possible experiments. *Zeitschrift für Naturforschung C*, 28:693, 1973.
- Holzappel G., Eberlein R., Wriggers P., and Weizsäcker H. Large strain analysis of soft biological membranes: Formulation and finite element analysis. *Comput. Methods Appl. Mech. Engrg*, 132:45–61, 1996.
- Lac E. and Barthès-Biesel D. Deformation of a capsule in simple shear flow: Effect of membrane prestress. *Physics of Fluids*, 17:072105, 2005.
- Le D., White J., Peraire J., Lim K., and Khoo B. An implicit Immersed Boundary method for three-dimensional membrane-fluid flow interactions. *Journal of Computational Physics*, 229:8427–8445, 2009.
- Li X. and Sankar K. Front tracking simulation of deformation and buckling instability of a liquid capsule enclosed by an elastic membrane. *Journal of Computational Physics*, 227:4998–5018, 2008.
- Lipowsky R. The conformation of membranes. *Nature*, 349:475–481, 1991.
- Ma L. and Klug W. Viscous regularization and r-adaptive remeshing for finite element analysis of lipid membrane mechanics. *J. Comput. Phys.*, 227:5816–5835, 2008.
- Mader M., Vitkova V., Abkarian M., Viallat A., and Podgorski T. Dynamics of viscous vesicles in shear flow. *The European Physical Journal E: Soft Matter and Biological Physics*, 19:389–397, 2006.
- Meyer M., Desbrun M., Schröder P., and Barr A. Discrete differential–geometry operators for triangulated 2–manifolds. *Visualization and Mathematics*, 3:34–57, 2002.
- Pozrikidis C., editor. *Modeling and Simulation of Capsules and Biological Cells*. Mathematical

- Biology and Medicine Series. Chapman & Hall/CRC, 2003.
- Ramanujan S. and Pozrikidis C. Deformation of liquid capsules enclosed by elastic membranes in simple shear flow: large deformations and the effect of fluid viscosities. *Journal of Fluid Mechanics*, 361:117–143, 1998.
- Scriven L. Dynamics of a fluid interface. *Chem. Eng. Sci.*, 12:98–108, 1960.
- Seifert U. Configurations of fluid membranes and vesicles. *Advances in Physics*, 46:13–137, 1997.
- Sui Y., Chen X., Chew Y., Roy P., and Low H. Numerical simulation of capsule deformation in simple shear flow. *Computers and Fluids*, 2009.
- Waugh R. Surface viscosity measurements from large bilayer vesicle tether formation. *Biophys. J.*, 38:29–37, 1982.